Copper (II) complex of salicylate phenanthroline induces the apoptosis of colorectal cancer cells, including oxaliplatin-resistant cells

ZIXIN LIU[1], LIMEI FAN[1], DONGQIN NIU[1], MING CHEN[1], WEIRAN ZHANG[1], YUCHEN LIU[2,3], JINHUA XU[1,4] and DONG WANG[1]

[1]School of Medicine, Jianghan University; [2]Wuhan Institute of Biomedical Sciences, School of Medicine, Jianghan University; [3]Cancer Institute, School of Medicine, Jianghan University, Wuhan, Hubei 430056; [4]School of Life Science and Technology, Wuhan University of Bioengineering, Wuhan, Hubei 430415, P.R. China

Received January 19, 2023; Accepted July 5, 2023

DOI: 10.3892/or.2023.8607

Abstract. Oxaliplatin (Oxa) is one of the most effective chemotherapeutic drugs used in the treatment of colorectal cancer (CRC). However, the use of this drug is associated with severe side-effects and patients eventually develop resistance to Oxa. In recent years, copper complexes have been extensively investigated as substitutes for platinum-based drugs. Therefore, a number of copper complexes have also been developed for cancer therapy, such as copper (II) complex of salicylate phenanthroline [Cu(sal)(phen)]. In the present study, the antitumor activity and the related molecular mechanisms of Cu(sal)(phen) were examined in CRC cells. As compared with the chemotherapeutic drug, Oxa, Cu(sal)(phen) was more effective in inducing apoptosis and reactive oxygen species (ROS) production, and in decreasing mitochondrial membrane potential in the CRC cell lines, HCT116 and SW480. In addition, the expression of the apoptosis-related proteins, Bcl-2 and survivin, and those of the upstream regulators, p-JAK2 and p-STAT5, were significantly decreased in the two cell lines following treatment with Cu(sal)(phen). Furthermore, the efficacy of the complex against CRC was found to be excellent in an animal model. The results of immunohistochemical analysis revealed that the expression levels of Bcl-2, survivin and Ki-67 in tumor tissues were decreased following Cu(sal)(phen) treatment. The antitumor mechanisms underlying Cu(Sal)(phen) treatment were the induction of ROS generation, the inhibition of the JAK2/STAT5 signaling pathway and the downregulation of the expression of anti-apoptotic proteins, such as Bcl-2 and survivin. On the whole, the findings of the present study indicated that Cu(sal)(phen) effectively inhibited the viability and proliferation of HCT116 and SW480 CRC cells; in the future, the authors aim to conduct further experiments in future studies to provide more evidence that supports the development of Cu(sal)(phen) as a therapeutic agent for CRC.

Correspondence to: Professor Jinhua Xu, School of Life Science and Technology, Wuhan University of Bioengineering, 1 Han Shi Road, Yangluo Economic Development Zone, Wuhan, Hubei 430415, P.R. China
E-mail: xu5520@gmail.com

Dr Dong Wang, School of Medicine, Jianghan University, 8 Sanjiaohu Road, Wuhan Economic and Technological Development Zone, Wuhan, Hubei 430056, P.R. China
E-mail: wangdong@jhun.edu.cn

Key words: copper (II) complex of salicylate phenanthroline, colorectal cancer cells, apoptosis, reactive oxygen species, xenograft tumor, JAK2/STAT5 pathway

Introduction

The onset of colorectal cancer (CRC) is relatively insidious, with a tendency for metastasis; a number of patients with CRC also have a poor prognosis, which has contributed to the increase in the CRC mortality rates to the second highest globally among all cancer types (1). Currently, the treatment of advanced-stage CRC is mainly limited to chemotherapy with cytotoxic agents, including oxaliplatin (Oxa) (2), irinotecan and 5-fluorouracil. Oxa has a high affinity for DNA and promotes cell apoptosis through the formation of platinum-DNA adducts (3,4). OXA has been proven to be the first metal coordination complex for the treatment of CRC (5) and is one of the most effective chemotherapeutic drugs. However, the long-term use of Oxa can lead to drug resistance (6), as well as to severe side-effects, such as neurotoxicity and hepatotoxicity (7,8). Therefore, the identification of novel compounds to meet the needs of OXA-resistant or OXA-intolerant patients is of utmost importance (6).

In recent years, a number of copper complexes have been developed, whose mechanisms of action are distinct from current platinum-based drugs (9,10), including the induction of reactive oxygen species (ROS) (11-13), DNA cleavage (10,12,14), ferroptosis (15), cell cycle blockage (11) and ubiquitin-proteasome system inhibition (16). Among these mechanisms, intracellular ROS generation has been reported most frequently. ROS comprises a large class of

unstable molecules that contain oxygen often being generated as natural by-products, with the mitochondria being considered as the prime source of endogenous ROS (17,18). ROS play a pivotal role in regulating and triggering apoptosis, thereby modulating cancer cell proliferation, survival and drug resistance (17). Tumor cells can activate the ROS scavenging system to counteract ROS damage and further resist cell apoptosis, which contributes to malignant transformation, metastasis and resistance to anticancer drugs. Therefore, it is crucial to understand the complex (oxidation-reduction) REDOX process in cancer cells and its underlying mechanisms, which can help identify more effective strategies with which to eliminate cancer cells and overcome the limitations of Oxa (19,20).

Cancer treatment can also be achieved by controlling the growth of cancer cells or by promoting cell death (21) and common therapeutic strategies include the activation of pro-apoptotic molecules or the inhibition of anti-apoptotic molecules. Bcl-2 protein family proteins are pivotal regulators of cell survival (22,23). Survivin, a member of the family of inhibitory apoptosis proteins (IAPs), is tumor-specific and is not expressed in normal tissues or is expressed at low levels. In addition, Bcl-2 and survivin are critical anti-apoptotic proteins that promote cell survival through multiple pathways, including maintaining the integrity of the mitochondria (22) and inhibiting the activity of the terminal effector enzymes, caspase-3 and caspase-7 (24). Previous studies have attempted to target Bcl-2 (25) and survivin (26) to promote cancer cell apoptosis.

Among the copper complexes that have been shown to exert significant inhibitory effects on tumor cells, copper (II) complexes containing 1,10-phenanthroline ligand (27) are among the extensively studied. In a previous study, it was demonstrated that copper (II) complex of salicylate phenanthroline [Cu(sal)(phen)] has prominent antitumor potential against triple-negative breast cancer *in vitro* and *in vivo* (28). Few studies (9,19) involving copper (II) complexes against CRC have been reported in the literature. Therefore, the effects of Cu(sal)(phen) on CRC cells were investigated in the present study, demonstrating the excellent efficacy of this complex against CRC *in vivo*.

Materials and methods

Cells, cell culture and reagents. To validate the effects of Cu(sal)(phen) on CRC, two human primary adenocarcinoma colon cancer cell lines, SW480 and HCT116, whose tumor biology has been extensively studied in the literature (29), were selected for use in the present study. Since these cells are derived from two different patients with CRC, the two investigated cell lines exhibit some differences at the genetic level (30), which made the results more reliable to a certain extent. The HCT116 (CCL-247EMT) and SW480 (CCL-228) human CRC cell lines were obtained from The Cell Bank of Type Culture Collection of the Chinese Academy of Sciences and cultured in DMEM containing 10% FBS and 1% penicillin/streptomycin (all purchased from Hyclone; Cytiva) at 37˚C in an atmosphere of 5% CO_2. Cu(sal)(phen) and Oxa were provided by Hubei Dinglong Chemical Co., Ltd. and Selleck Chemicals, respectively.

Cell viability and colony formation assay. Cell viability was determined using 3-(4,5-dimethylthiazol-2-yl)-5-(3-carboxym ethoxyphenyl)-2-(4-sulfophenyl)-2H-tetrazolium (MTS) assay with CellTiter 96® AQueous One Solution Cell Proliferation Assay (Promega Corporation). Accordingly, the cells were grown in 96-well plates overnight and then treated with Cu(sal)(phen) and Oxa at various concentrations (1, 2.5, 5, 10, 25 μM) with dimethyl sulfoxide (DMSO) used as the control. Following 48 or 72 h of treatment, MTS was added to the plates and incubated for 3 h at 37˚C. Subsequently, the optical density was recorded at 492 nm using a Synergy 2 plate reader (BioTek Instruments, Inc.). The half-maximal inhibitory concentration (IC_{50}) was calculated based on the percentage decrease in the optical density at 492 nm relative to the control group using GraphPad prism 7.0 (Dotmatics).

A colony formation assay was conducted in order to evaluate cell proliferation. Briefly, the cells were seeded in six-well plates at a density of 500 cell/well for 48 h, followed by treatment with 1 and 2.5 μM Cu(sal)(phen) and Oxa for 14 days. The medium was changed every 3 days, and the colonies were fixed with 4% paraformaldehyde for 50 min at room temperature. Finally, 0.5% crystal violet dye (Sinopharm Chemical Reagent Co., Ltd.) for 50 min was used to stain cell colonies, and the colonies were counted using the Fiji (ImageJ 2.1.0) software (National Institutes of Health).

Apoptosis assay. An Annexin V-FITC/PI Apoptosis Assay kit (Beijing Zoman Biotechnology Co., Ltd.) was used to examine cell apoptosis after HCT116 and SW480 cells were treated with Cu(sal)(phen) (25 μM) or Oxa (25 μM) with or without 20 μM carbobenzoxy-valyl-alanyl-aspartyl-[O-methyl]-fluoromethylketone (Z-VAD-FMK; GlpBio) solution in DMSO at 37˚C. In brief, the cells were collected (200 x g, 5 min, 4˚C) following treatment and staining with Annexin V-FITC and propidium iodide (PI) for 15 min in the dark. The samples were then measured using a BD Accuri™ C6 Flow Cytometer (BD Biosciences), and the data were analyzed using FlowJo 10.6.2 software (BD Biosciences).

ROS accumulation assay. A Reactive Oxygen Species Assay kit (Beyotime Institute of Biotechnology) was used to detect ROS accumulation. According to the manufacturer's instructions, the cells were pre-treated with or without *N*-acetylcysteine (NAC; 5 mM, Selleck Chemicals) or glutathione (GSH; 1 mM, GlpBio) for 1 h at 37˚C prior to the addition of Cu(sal)(phen) and harvested (200 x g, 5 min, 4˚C), followed by staining with 2',7'-dichlorofluorescein diacetate (DCFH-DA) for 20 min at 37˚C. Samples were detected, and the data were analyzed using a BD Accuri™ C6 Flow Cytometer (BD Biosciences) and FlowJo 10.6.2 software (BD Biosciences), respectively.

Mitochondrial membrane potential ($\Delta\psi m$) assay. The depolarization of $\Delta\psi m$ was measured using a Mitochondrial Membrane Potential Assay kit with JC-1 (Bestbio). According to the manufacturer's instructions, the treated and collected cells were stained with JC-1 for 30 min at 37˚C and observed using a flow cytometer (BD Biosciences). Finally, the data were gathered and analyzed using FlowJo 10.6.2 software (BD Biosciences).

Western blot analysis. Cells treated with Cu(sal)(phen) and Oxa were lysed with RIPA lysis buffer (Beyotime Institute of Biotechnology) supplemented with complete protease inhibitor cocktail (Roche Applied Science) and phenylmethane sulfonyl fluoride. The protein concentration was determined using the BCA method. Following heating for 10 min; at 95˚C in loading buffer, 25 μg proteins were separated by 10% SDS-PAGE and transferred onto a PVDF membrane blocked with a blocking buffer [Odyssey Blocking Buffer (PBS); LI-COR Biosciences] for 1 h at room temperature. Western blot analysis was performed using primary and secondary antibody incubation. Subsequently, blots were acquired using Odyssey SA (LI-COR Biosciences) and images analyzed using Image Studio ver 5.2 software (LI-COR Biosciences). Primary antibody incubation was carried out overnight at 4˚C. The following primary antibodies were used: Anti-Bcl-2 (1:1,000, cat. no. ab32124; Abcam), anti-survivin (1:500, cat. no. 2808S; Cell Signaling Technology, Inc.), anti-cleaved poly (ADP-ribose) polymerase (PARP; 1:300, cat. no. 9541S; Cell Signaling Technology, Inc.), anti-γ-H2A histone family member X (γ-H2AX; 1:5,000, cat. no. ab81299; Abcam), anti-caspase-3 (1:1,000, cat. no. 9662s; Cell Signaling Technology, Inc.), anti-cleaved casepase-3 (1:1,000, cat. no. 9664; Cell Signaling Technology, Inc.), anti-p-JAK2 (1:1,000, cat. no. 3771s; Cell Signaling Technology, Inc.), anti-p-STAT3 (1:500, cat. no. ab76315; Abcam), anti-p-STAT5 (1:1,000, cat. no. 68000-1-Ig; ProteinTech Group, Inc.) and anti-actin (1:2,000, cat. no. EM21002; Huabio). The following secondary antibodies were used (incubation for 1 h at room temperature): Odyssey Blocking Buffer (PBS), fluorescently-labeled goat anti-rabbit (cat. no. 926-32211) or goat anti-mouse antibody (cat. no. 926-32210) (both 1:10,000; LI-COR Biosciences).

Xenograft tumor experiment. All animal experiments were carried out in accordance with the protocols of the Institutional Animal Care and Use Committee of Jianghan University. The animal experiments followed the rules of the Animal Ethics Committee of Jianghan University (Wuhan, China) and were performed in accordance with relevant guidelines and regulations, including the ARRIVE guidelines (ethics permission no. JHDXLL:2019-001). BALB/c-nu female mice [5 weeks old; specific pathogen-free (SPF); Beijing, n=25) Biotechnology Co., Ltd.] were domesticated for 1 week and then used to construct a xenograft tumor model. All mice were maintained in a specific pathogen-free state, with a regulated 12-h light/dark cycle, and constant temperature (22±2˚C) and relative humidity (50±10%). HCT116 cells ($5x10^6$) were suspended in 100 μl medium containing 50% Matrigel and injected subcutaneously into the right flanks of the mice. After the tumors grew to ~100 mm^3, the mice selected according to the criteria (n=21, tumor volume ~100 mm^3; 4 mice were excluded as their tumor size exceeded the standard deviation of mouse tumor volume by 3-fold) were randomly divided into three groups (n=7) and intraperitoneally administered either 70% DMSO solution in saline (control solution) as the vehicle control, Cu(sal)(phen) (5 mg/kg in control solution) or Oxa (5 mg, in saline) every other day. The mouse tumor volumes and body weights were monitored every other day for 18 days. Tumor volumes were calculated based on the following formula: $V=0.5 \times l \times w^2$, where l is the length (mm), w is the width (mm), and V is the volume of tumor. The mice were sacrificed with isoflurane. Briefly, the mice were placed in a plexiglass chamber with 5% isoflurane until respiration ceased. The death of the mice was confirmed by a lack of active paw reflex and no heartbeat. The tumor weights were recorded and the tumor tissues were fixed in Bouin's (100%) fixative solution (Phygene) for 48 h at room temperature. The tumor tissues were then embedded into paraffin blocks. After sectioning the tissue blocks into 4-μm-thick slices, the sections were stained with a hematoxylin and eosin (H&E) staining solution (Wuhan POWERFUL Biotechnology Co., Ltd.; http://boerfu.net/) for 4 min 15 sec at room temperature. An upright microscope (ECLIPSE Ni-U, Nikon Corporation) was used to observed the sections and the images were captured and analyzed at x200 magnification using NIS-Elements D software (5.3.00, Nikon Corporation).

For immunohistochemistry (IHC), the aforementioned tissue sections (4-μm-thick) were deparaffinized with xylene, rehydrated with a decreasing ethanol series, and then washed three times with distilled water for 5 min at room temperature. Subsequently, these sections were blocked using 3% BSA (cat. no. A8010, Beijing Solarbio Science & Technology Co., Ltd.) for 30 min at room temperature. The slides were then incubated with anti-Ki67 (1:1,000, cat. no. ab32124; Abcam), anti-Bcl-2 (1:100, cat. no. ab32124; Abcam) and anti-survivin (1:400, cat. no. 2808S; Cell Signaling Technology, Inc.) antibodies overnight at 4˚C. The sections were then stained with DAB (cat. no. K3468, Dako; Agilent Technologies, Inc.) at room temperature and the color development time was controlled using a microscope by the positive brownish yellow color and the section was washed with tap water to terminate the color development. Subsequently, the nuclei were counterstained with hematoxylin (cat. no. BH0001, Wuhan POWERFUL Biotechnology Co., Ltd.; http://boerfu.net/) at room temperature for 3 min. Finally, the sections were dehydrated with increasing concentrations of ethanol and xylene. A PANNORAMIC Digital Slide Scanner (3D Histech) were used to scan the sections. The images were analyzed using the Fiji (ImageJ 2.1.0) (National Institutes of Health) and CaseViewer (2.2, 3D Histech) software.

Furthermore, humane endpoints were set when the tumor diameter >20 mm, tumor necrosis, ulceration, or tumor infection. Mice that reached the humane endpoint were euthanized. No mice were sacrificed due to reaching the humane endpoints.

Statistical analysis. Results from three independent experiments were presented as the mean ± SEM. One- or two-way ANOVA (Tukey's multiple comparisons test) were used to compare the differences among groups. Statistical differences were evaluated using GraphPad prism 7.0 (GraphPad Software, Inc.). $P<0.05$ was considered to indicate a statistically significant difference.

Results

Cu(sal)(phen) inhibits CRC cell viability and proliferation. To evaluate the potential effect of Cu(sal)(phen) on CRC cells, an MTS assay was conducted with various concentrations of Cu(sal)(phen). Oxa was used as a positive control. Cu(sal)(phen) displayed a potent ability to inhibit cell viability in a

concentration- and time-dependent manner in the HCT116 and SW480 cell lines (Fig. 1A). Oxa exhibited a moderate inhibitory effect on the viability of HCT116 cells, even though it is one of the most commonly used chemotherapeutic drugs for the clinical treatment of CRC (3,7). Furthermore, Oxa had a minimal inhibitory effect on the SW480 cell line, confirming that it was indeed an Oxa-resistant cell line, as previously reported (31). However, the SW480 cells were sensitive to Cu(sal)(phen) treatment (Fig. 1A). The IC_{50} values of Cu(sal)(phen) at 48 and 72 h were 4.28 and 3.48 μM, respectively, while the IC_{50} values of Oxa at 48 and 72 h were >100 and 66.55 μM, respectively. These findings suggested that Cu(sal)(phen) was more effective than Oxa in inhibiting CRC cell viability.

To further validate the inhibitory effects of Cu(sal)(phen) on CRC cell viability, a colony formation assay was performed. As shown in Fig. 1B, the proliferation was markedly lower than that of the control groups in the Cu(sal)(phen)-treated HCT116 and SW480 cells. Oxa treatment exerted similar effects as Cu(sal)(phen) treatment. The aforementioned results demonstrated that Cu(sal)(phen) effectively inhibited CRC cell growth *in vitro*.

Cu(sal)(phen) induces CRC cell apoptosis. Since Cu(sal)(phen) was more effective than Oxa in decreasing cell viability, the role of Cu(sal)(phen) in inducing cell apoptosis was then investigated. The HCT116 and SW480 cells were treated with various concentrations of Cu(sal)(phen) or Oxa for 24 h, and cell apoptosis was then measured using an apoptosis assay. As shown in Fig. S1, Cu(sal)(phen) effectively induced the apoptosis of the two cell lines in a concentration-dependent manner. At a concentration of 25 μM, the apoptotic rate was as high as 26.4% (HCT116 cells) and 25.8% (SW480 cells). However, the apoptotic rate of the two cell lines only remained at ~10% following treatment with 25 μM Oxa (Fig. 2A). Using an apoptosis inhibitor, Z-VAD-FMK, it was found that pre-treatment of the CRC cells with 20 μM Z-VAD-FMK for 1 h prior to the addition of Cu(sal)(phen) significantly attenuated the apoptosis of both the HCT116 and SW480 cells (Fig. 2B and C). These results indicated that Cu(sal)(phen) was more effective than Oxa in promoting the apoptosis of the two selected CRC cell lines at a concentration of 25 μM.

Cu(sal)(phen) promotes apoptosis through ROS generation. A number of reports on copper (II) complexes have revealed the crucial role of ROS in promoting cell apoptosis (13,20,27,32). In order to elucidate the mechanisms through which Cu(sal)(phen) induces higher levels of apoptosis than Oxa, a ROS generation assay was conducted. The results shown in Fig. 3A revealed a significantly higher generation of ROS in both CRC cell lines treated with Cu(sal)(phen), as compared with the control group. The changes in ROS generation were 5.5- and 2.7-fold in the HCT116 and SW480 cells, respectively. Pre-treatment with the ROS scavenger, NAC (33), significantly reduced ROS generation in both the HCT116 and SW480 cell lines (Fig. 3A). By comparison, ROS production did not differ significantly compared to the control following treatment of the two CRC cell lines with Oxa (Fig. S2A). To determine the association between ROS production and cell apoptosis, NAC was added to the CRC cells to reassess Cu(sal)(phen)-mediated apoptosis. As was expected, the addition of NAC to the Cu(sal)(phen)-treated HCT116 cells led to a decreased level of apoptosis, as compared with the Cu(sal)(phen) group (Fig. 3B). Unexpectedly, the combination of NAC and Cu(sal)(phen) markedly increased SW480 cell apoptosis (Fig. S2B). Another antioxidant, GSH, was used to determine Cu(sal)(phen)-induced ROS production and apoptosis. As shown in Fig. 3A and C, GSH attenuated Cu(sal)(phen)-induced ROS generation and SW480 cell apoptosis. It was thus found that Cu(sal)(phen) initiated apoptosis through ROS production.

Cu(sal)(phen) induces the depolarization of Δψm in CRC cells. Mitochondria are considered to be a major source of ROS (17,18,34), which is closely associated with cell apoptosis. In addition, cell apoptosis is often accompanied by Δψm depolarization. For that reason, in the present study, a Δψm assay was performed, and there was a notable decrease in Δψm in the HCT116 and SW480 cells following treatment of the two cell lines with 25 μM Cu(sal)(phen) (Fig. 3D). Pretreatment with NAC partially reversed Δψm reduction in Cu(sal)(phen)-treated HCT116 cells. In addition, GSH treatment also reversed the reduction in Δψm in the Cu(sal)(phen)-treated SW480 cells (Fig. 3D). In line with the results of ROS assay, the Δψm of the two cell lines treated with Oxa was not markedly altered compared with the controls (Fig. S3). Thus, as demonstrated by the results, the Cu(sal)(phen)-induced apoptosis was closely associated with the release of ROS by the mitochondria.

Cu(sal)(phen)-induced cell death is dependent on the regulation of apoptosis-related proteins. In order to further elucidate the mechanisms of Cu(sal)(phen)-induced cell death, a variety of proteins involved in apoptosis were detected using western blot analysis. Bcl-2 is a member of the Bcl-2 family which confers a survival advantage to cancer cells by maintaining mitochondrial integrity (22,35). Bcl-2 expression in the HCT116 and SW480 cells was downregulated following treatment with Cu(sal)(phen) at 25 μM compared with the control group, as shown in Fig. 4A. However, Bcl-2 expression in the HCT116 cells was not decreased in the Oxa group. In the SW480 cells treated with Oxa, Bcl-2 expression only decreased to a level comparable to that of Cu(sal)(phen). Unlike Bcl-2, survivin belongs to the IAP family; it is overexpressed in cancer cells, but rarely in normal adult tissues and plays a crucial anti-apoptotic role in cancer cells (24,36). Survivin expression was downregulated by Cu(sal)(phen) at a concentration of 25 μM, but not by Oxa in the two CRC cell lines, as compared with the control (Fig. 4A and B).

PARP is a substrate of caspases, and its product, cleaved PARP, is generally used to detect cancer cell apoptosis (37). The levels of cleaved PARP were increased in both CRC cell lines in the Cu(sal)(phen) group (Fig. 4A and B). Consistent with this observation, the levels of cleaved caspase-3 were increased in both cell lines following treatment with Cu(sal)(phen). In order to elucidate the association between Cu(sal)(phen) and apoptosis, the level of γ-H2AX, a biomarker of DNA double-strand breaks (DSBs) often caused by ROS (38), was analyzed. γ-H2AX expression was significantly increased in both the HCT116 and SW480 cells following treatment with Cu(sal)(phen) compared with the control.

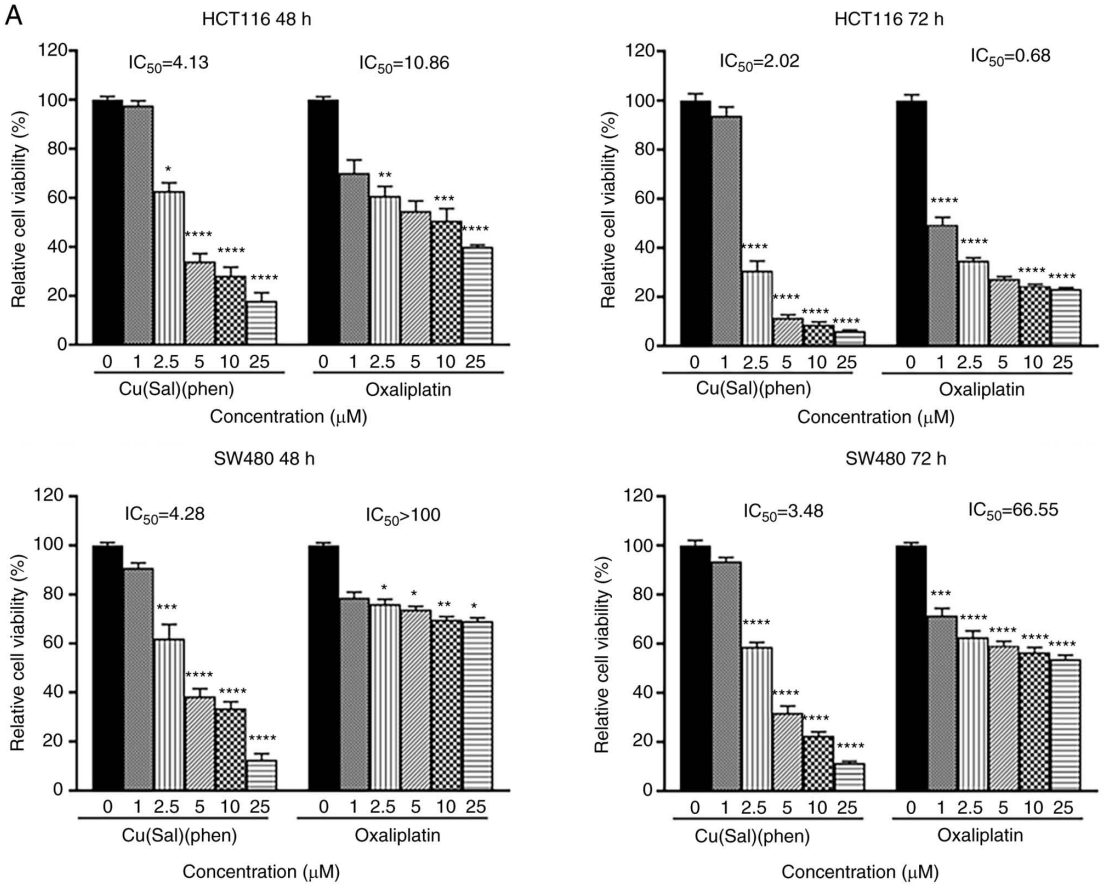

Antitumor activity IC_{50} (μM)±SEM

	Cu(Sal)(phen)		Oxaliplatin	
	48 h	72 h	48 h	72 h
HCT116	4.13±0.68	2.02±0.16	10.86±4.96	0.68±0.24
SW480	4.28±0.67	3.48±0.32	>100	66.55±46.56

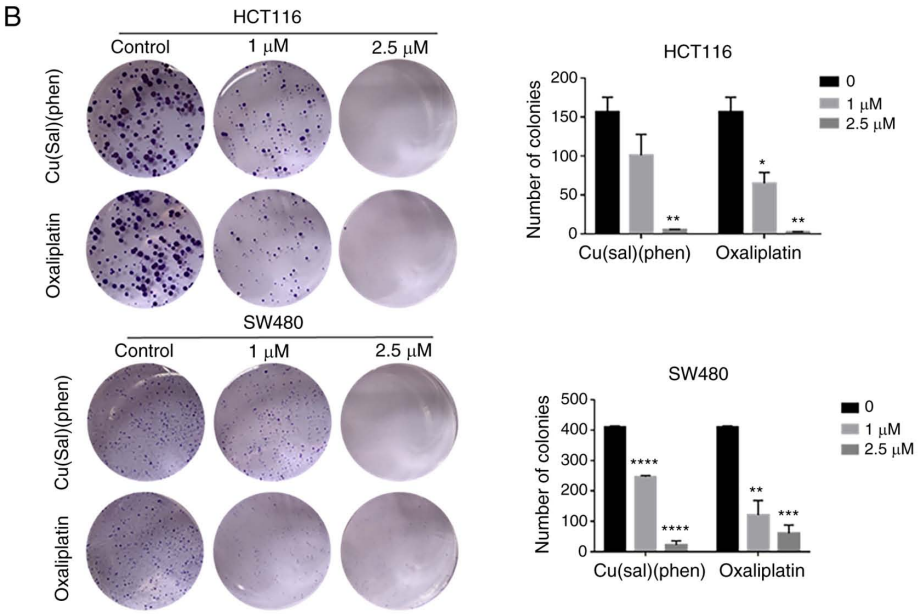

Figure 1. Cu(sal)(phen) inhibits CRC cell growth. (A) HCT116 and SW480 cells were treated with 0-25 μM Cu(sal)(phen), and cell viability was measured using an MTS assay at the indicated time points. (B) Cell proliferation was analyzed using a colony formation assay. Cells were seeded in six-well plates at a density of 500 cells/well for 48 h followed by treatment with Cu(sal)(phen) and Oxa for 14 days. The medium was changed every 3 days and the colonies were fixed with 4% paraformaldehyde and then stained with 0.5% crystal violet dye. At the end of the experiment, the colonies were counted using Fiji (ImageJ 2.1.0) software. These results are presented as the mean of three independent experiments performed in triplicate. The bars represent the mean ± SD. *P<0.05, **P<0.01, ***P<0.001 and ****P<0.0001, compared to the control (no treatment). Cu(sal)(phen), copper (II) complex of salicylate phenanthroline; CRC, colorectal cancer; MTS, 3-(4,5-dimethylthiazol-2-yl)-5-(3-carboxymethoxyphenyl)-2-(4-sulfophenyl)-2H-tetrazolium; Oxa, oxaliplatin.

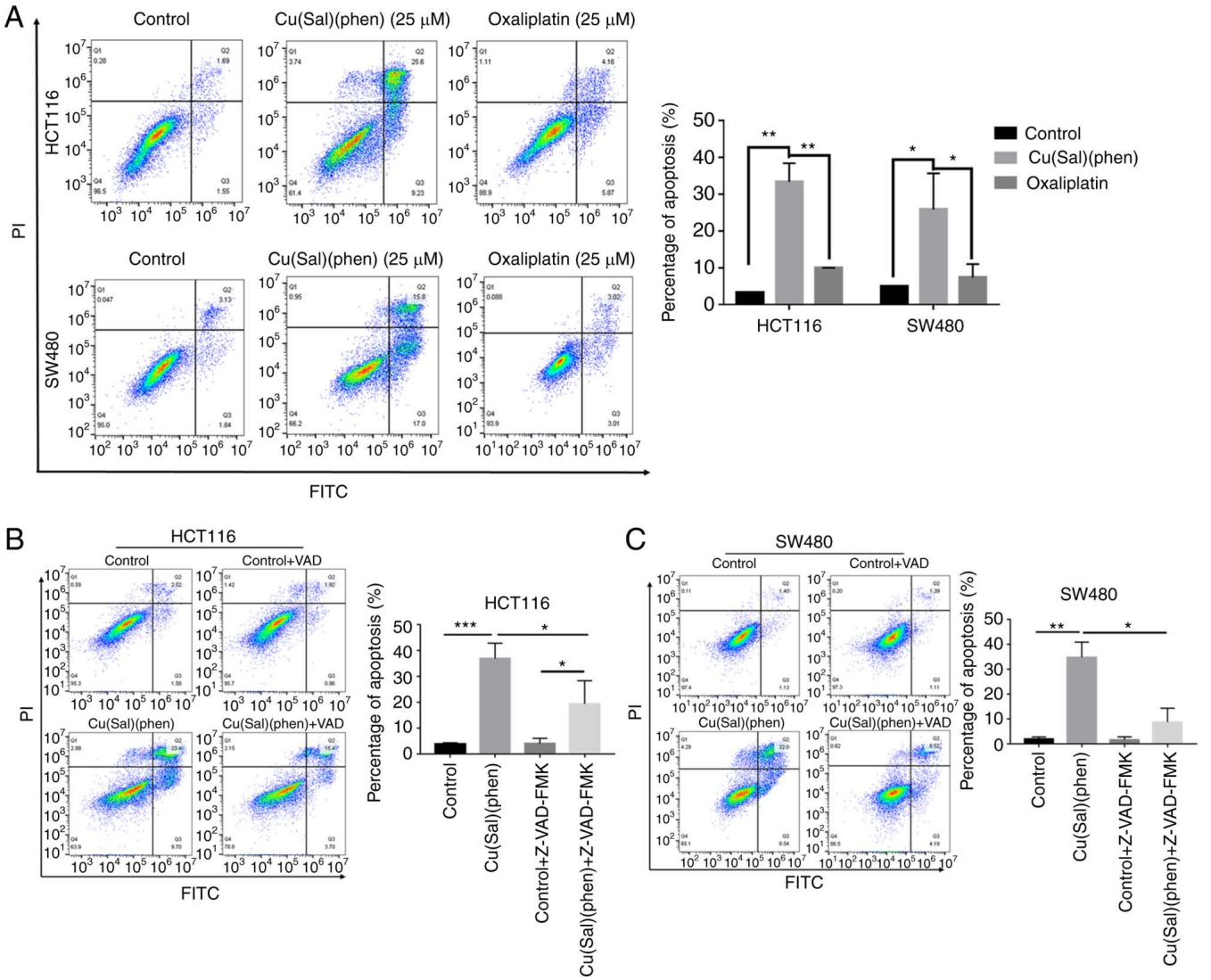

Figure 2. Cu(sal)(phen) induces CRC cell apoptosis. (A) HCT116 and SW480 cells were treated with 25 μM Cu(sal)(phen) or oxaliplatin for 24 h, and apoptosis was assessed using flow cytometry following Annexin V/PI double staining. (B) The HCT116 cells were treated with 20 μM Z-VAD-FMK for 1 h prior to the addition of Cu(sal)(phen), and apoptosis was then analyzed using flow cytometry. (C) The SW480 cells were treated with 20 μM Z-VAD-FMK for 1 h prior to the addition of Cu(sal)(phen) and then apoptosis was analyzed by flow cytometry. The results are presented as the mean of three independent experiments. Bars represent the mean ± SD. *P<0.05, **P<0.01 and ***P<0.001. Cu(sal)(phen), copper (II) complex of salicylate phenanthroline; CRC, colorectal cancer; PI, propidium iodide; Z-VAD-FMK, carbobenzoxy-valyl-alanyl-aspartyl-[O-methyl]-fluoromethylketone.

As a drug which directly acts on DNA, Oxa was found to upregulate γ-H2AX expression in the two CRC cell lines; however, its effect was less prominent compared with that of Cu(sal)(phen).

The JAK2/STATs signaling pathway (33) is involved in the regulation of apoptosis through Bcl-2 in cancer cells. Therefore, the present study examined whether Cu(sal)(phen) can affect the JAK2/STAT5 pathway in CRC cells. As shown in Fig. 4C and D, the expression of p-STAT5 and p-JAK2 was significantly inhibited following treatment of the HCT116 and SW480 cells with 25 μM Cu(sal)(phen), while the expression of p-STAT5 and p-JAK2 remained unaltered following treatment with 25 μM Oxa. The level of p-STAT3 remained unaltered following treatment of the two CRC cell lines with Cu(sal)(phen) or Oxa. These results suggested that Cu(sal)(phen) induces CRC cell apoptosis by downregulating the JAK2/STAT5 pathway.

Cu(sal)(phen) suppresses tumor growth in the HCT116 cell xenograft model. Due to the results obtained from the *in vitro* experiments, the antitumor effect of Cu(sal)(phen) was investigated *in vivo* using a HCT116 cell xenograft model. The tumor volumes and body weights of the mice were recorded following the first administration of the drugs and until the mice were euthanized. The tumor growth curves illustrated in Fig. 5A suggested that Cu(sal)(phen) and Oxa markedly attenuated tumor growth in the mice following 18 days of treatment, as compared with the control group. Of note, the antitumor effects of Cu(sal)(phen) were almost comparable to those of Oxa. The results were further supported by the images and weights of the tumors (Fig. 5C and D). There was no statistically significant difference in body weight among the three groups of mice (Fig. 5B). This suggested that Cu(sal)(phen) can effectively suppress HCT116 cell xenograft tumor growth without any evident toxicity *in vivo*.

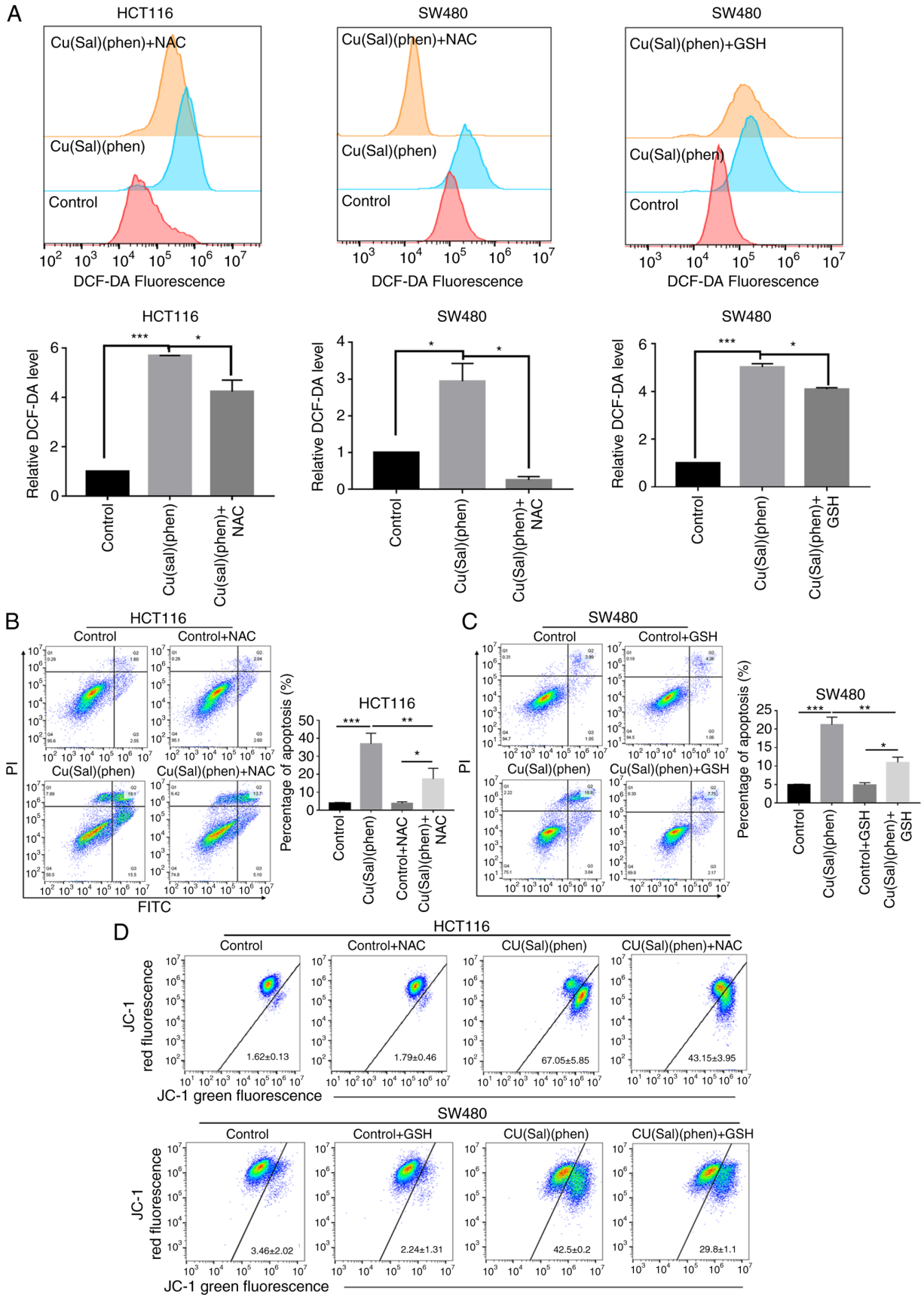

Figure 3. Cu(sal)(phen) induces apoptosis and decreases Δψm through ROS generation. (A) The ROS level was detected using flow cytometry in HCT116 and SW480 cells treated with Cu(sal)(phen), Cu(sal)(phen) plus NAC and Cu(sal)(phen) plus GSH, respectively. The fold change in DCFH-DA intensity is shown in the bottom panels. (B) HCT116 cell apoptosis was analyzed using flow cytometry following treatment with Cu(sal)(phen) with or without NAC. (C) SW480 cell apoptosis was analyzed using flow cytometry following treatment with Cu(sal)(phen) with or without GSH. (D) The Δψm of HCT116 and SW480 cells was analyzed using JC-1 staining and flow cytometry following treatment with Cu(sal)(phen) with or without NAC/GSH. *P<0.05, **P<0.01 and ***P<0.001. Cu(sal)(phen), copper (II) complex of salicylate phenanthroline; Δψm, mitochondrial membrane potential; ROS, reactive oxygen species; NAC, N-acetylcysteine; GSH, glutathione; DCFH-DA, dichlorofluorescein diacetate.

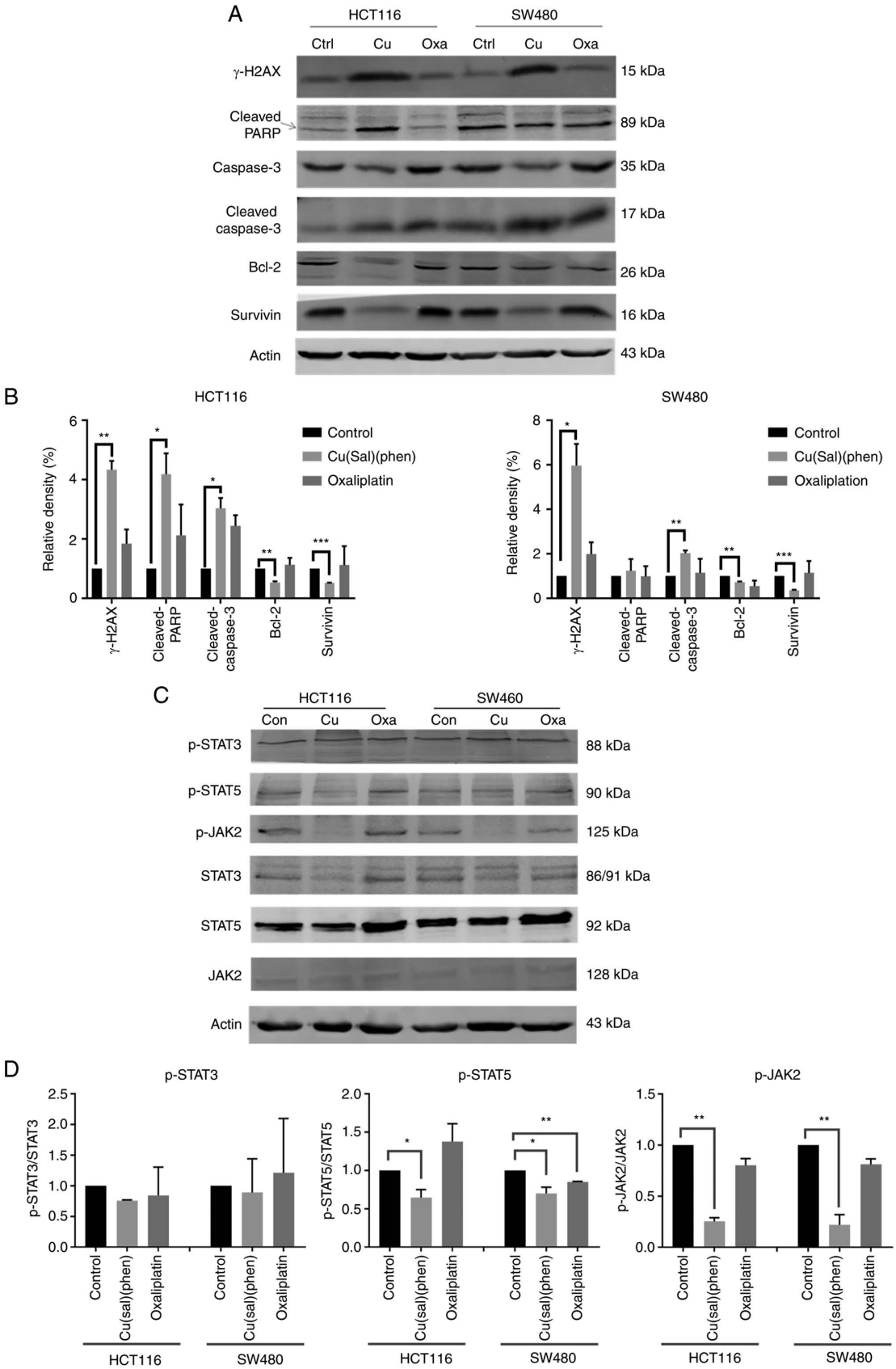

Figure 4. Cu(sal)(phen) induces CRC cell apoptosis by downregulating the JAK2/STAT5 pathway. Protein expression was examined using western blot analysis following treatment of the HCT116 or SW480 cells with 25 μM Cu(sal)(phen) or oxaliplatin. DMSO was used as a control. Actin was used as a loading control. (A) Representative western blots of γ-H2AX, c-PARP, caspase-3, c-caspase-3, Bcl-2 and survivin in HCT116 and SW480 cells. (B) Quantitative analysis of the western blots of HCT116 and SW480 cells. The densities of the target bands were scanned, and values were normalized to those of actin. (C) Representative western blots of p-STAT3, p-STAT5 and p-JAK2 in HCT116 and SW480 cells. (D) The quantitative analysis of the western blots in (C) was performed as described in (B). The results are presented as the mean of two independent experiments. Bars represent the mean ± SD. *P<0.05, **P<0.01 and ***P<0.001. Cu(sal)(phen), copper (II) complex of salicylate phenanthroline; CRC, colorectal cancer; DMSO, dimethyl sulfoxide; γ-H2AX, H2A histone family member X; c-PARP, cleaved poly(ADP-ribose) polymerase.

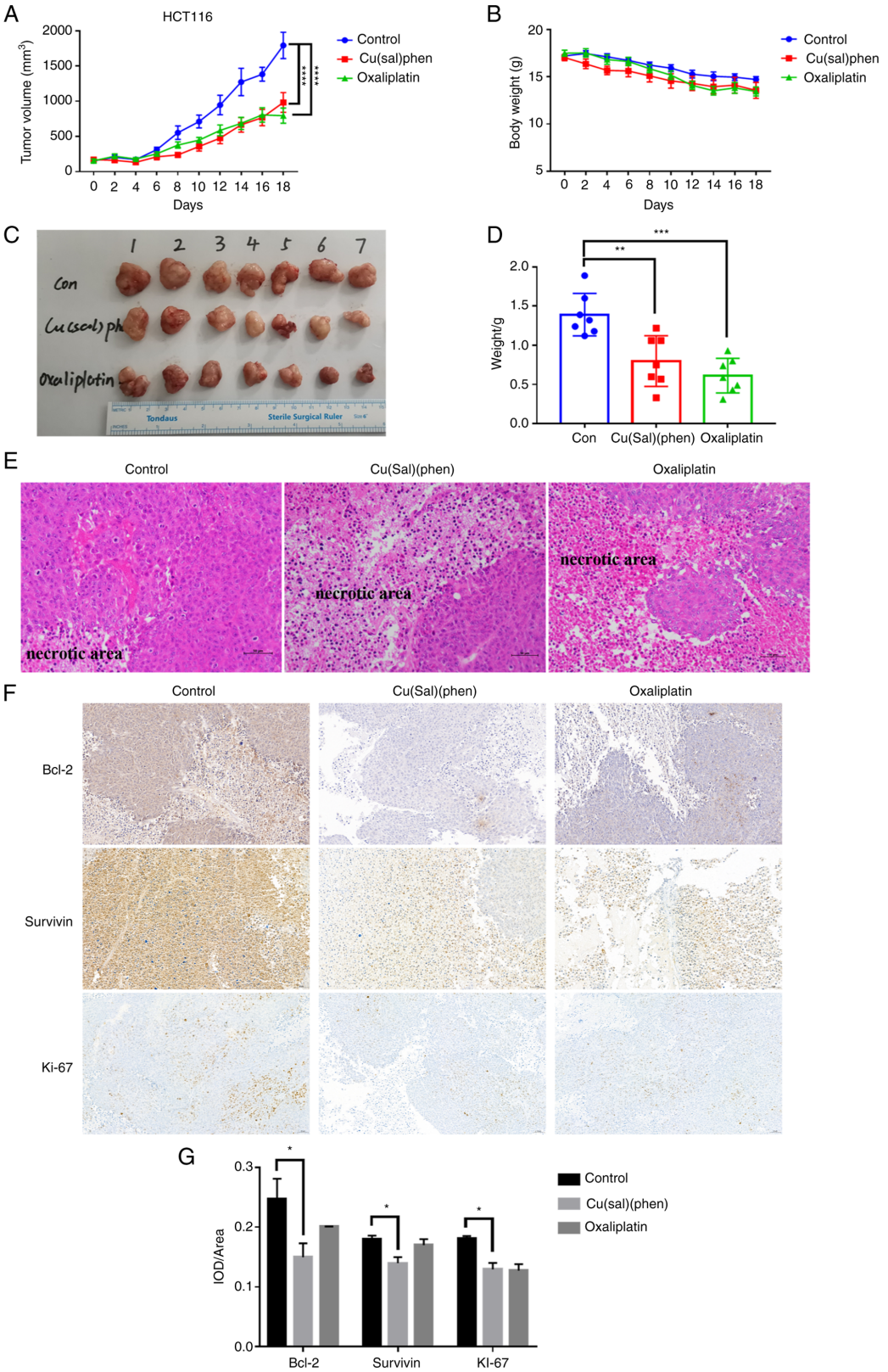

Figure 5. Cu(sal)(phen) suppresses tumor growth in the HCT116 cell xenograft model. The mice were injected intraperitoneally every 2 days with 0.1 ml DMSO or 5 mg/kg Cu(sal)(phen) or 5 mg/kg Oxa. Tumor size and body weight were measured every other day throughout the experiments. After 18 days of treatment, the mice were euthanized, and the tumors were fixed, sectioned and stained with H&E. (A) Tumor volume for the tumor-bearing mice is presented as the mean per group (n=7). ****P<0.0001, between the treated and control groups. (B) There was no significant difference in the mean body weight between the mice in the treatment and control groups. (C) Images of the tumors at the end of the study period in each group. (D) Tumor weights in each group were measured at the end of the treatment. (E) H&E staining of tumor specimens from the mice injected with DMSO or Cu(sal)(phen) or Oxa. Magnification, x200. (F) Cu(sal)(phen) downregulated the levels of anti-apoptotic and proliferation-related proteins in xenograft tumors. Formalin-fixed, paraffin-embedded sections were stained with antibodies against Bcl-2, survivin and Ki-67. Magnification, x200. (G) Results of semi-quantitative analysis of immunohistochemistry images. The IOD (n=24) was measured using Image-pro plus 6.0 software (Media Cybernetics). Expression levels of all three proteins in the treated and control groups. *P<0.05, **P<0.01 and ***P<0.001. Cu(sal)(phen), copper (II) complex of salicylate phenanthroline; H&E, hematoxylin and eosin; DMSO, dimethyl sulfoxide; IOD, integrated optical density; Oxa, oxaliplatin.

To investigate the possible mechanisms of the antitumor effects of Cu(sal)(phen) *in vivo*, H&E staining and IHC of the tumors were performed. H&E staining revealed evident necrotic areas in the tumors from the drug-treated group that were not observed in the control tumors (Fig. 5E). Consistent with the results obtained *in vitro*, the levels of the two apoptotic proteins, Bcl-2 and survivin, were decreased, and the level of the proliferation marker, Ki-67, was decreased (Fig. 5F and G). Collectively, Cu(sal)(phen) inhibited tumor growth in the HCT116 cell xenograft model, and the mechanism of the antitumor activity appeared to involve the downregulation of Bcl-2 and survivin.

Discussion

Platinum-based metal complexes are widely used in the treatment of various solid tumors (39). However, their use is limited by drug resistance and significant side effects (40). Therefore, several non-platinum metal complexes have been investigated due to their novel antitumor mechanisms of action (40). The present study reported a copper (II) complex bearing salicylate and phenanthroline as ligands, abbreviated as Cu(sal)(phen), which could effectively mediate the apoptosis of HCT116 and SW480 CRC cell lines through the induction of ROS, mitochondrial depolarization and downregulation of the anti-apoptotic pathway of JAK2/STAT5. Cu(sal)(phen) exhibited the ability to induce the apoptosis of Oxa-sensitive cell line HCT116 and Oxa-resistant cell line SW480.

Triggering cell apoptosis through different mechanisms is a crucial strategy in the development of anti-neoplastics (41). Mitochondria are a major source of endogenous ROS (17,18,34) and play a central role in both extrinsic and intrinsic apoptotic pathways (42,43). The enhancement of ROS generation has been shown to promote apoptosis and mitochondrial depolarization in CRC cell lines (44). Furthermore, ROS production by the copper (II) complex has been demonstrated to play a pivotal role in cell death (9,32,45). Based on the aforementioned information, ROS production and mitochondrial depolarization mediated by Cu(sal)(phen) may be closely associated with Cu(sal)(phen)-induced apoptosis. The finding that Cu(sal)(phen)-mediated apoptosis was attenuated by NAC and Z-VAD-FMK provided further evidence of the association between apoptosis and ROS production. Given that ROS can lead to mitochondrial dysfunction in CRC cells (46), it was hypothesized that Cu(sal)(phen) may initiate apoptosis through the induction of ROS production that results in mitochondrial depolarization.

Cancer cells have a broad association with ROS, and ROS generated by metabolic abnormalities and carcinogenic signals can lead to an increased production of natural antioxidants (47). As a result, cancer cells are more dependent on the antioxidant system and more sensitive to exogenous ROS or antioxidant inhibitors. Adding exogenous ROS to further increase ROS production in cancer cells can cause ROS levels to increase to unacceptable levels, resulting in cell death. This provides a biochemical basis for designing therapeutic strategies that selectively kill cancer cells using ROS-mediated mechanisms (48). Of note, it was found that combined treatment with antioxidant NAC and Cu(sal)(phen) markedly enhanced SW480 cell apoptosis (data not shown). However, GSH attenuated the Cu(sal)(phen)-induced apoptosis of SW480 cells. Although the exact mechanisms involved remains unclear, the intracellular REDOX system is much more complex than was previously considered. Further studies are warranted to determine whether Cu(sal)(phen) can mediate the recently defined cuproptosis (49), that is not triggered by caspases and not attenuated by NAC.

Bcl-2 family proteins are pivotal regulators of cell apoptosis (22,23). In addition, Bcl-2 and survivin are critical anti-apoptotic members that promote cell survival through a number of mechanisms, such as maintaining the integrity of the mitochondria (22) and inhibiting the activity of terminal effector enzymes, caspase-3 and caspase-7 (24). Previous studies have tried to promote apoptosis by targeting Bcl-2 (25,50) and survivin (26,51). In line with these reports, the present study found that the Bcl-2 and survivin levels were downregulated by Cu(sal)(phen) in the HCT116 and SW480 cells *in vitro* and in the HCT116 cell xenograft model *in vivo*. Furthermore, the p-JAK2 and p-STAT5 levels were also downregulated following treatment of the two CRC cell lines with Cu(sal)(phen). STAT5 is a transcription factor that activates the transcription of Bcl-2 (52). Thus, it was inferred that Cu(sal)(phen) mediated CRC cell apoptosis not only by inducing ROS generation, but also by downregulating survivin, Bcl-2 and its upstream proteins, including p-JAK2 and p-STAT5.

In order to further confirm the antitumor efficacy of Cu(sal)(phen), the levels of the apoptotic marker, cleaved PARP, and the DSB marker, γ-H2AX, were examined in the HCT116 and SW480 cell lines. In addition, the proliferation marker, Ki-67, was examined in the HCT116 cell xenograft model. As was expected, treatment with Cu(sal)(phen) increased the levels of cleaved PARP and γ-H2AX that was triggered by DSBs *in vitro*, and further decreased the level of Ki-67 *in vivo*, suggesting that Cu(sal)(phen) exhibited good antitumor efficacy both *in vitro* and *in vivo*.

In conclusion, the findings of the present study suggest that Cu(sal)(phen) inhibits the proliferation and induces the apoptosis of CRC cells *in vitro*, while also inhibiting tumor growth *in vivo* in nude mice. In addition, Cu (sal) (phen) was shown to have a good safety profile in previous *in vivo* experiments on Balb/c mice (53). The underlying mechanisms of Cu(sal)(phen) treatment involve the induction of ROS generation, the inhibition of the JAK2/STAT5 signaling pathway and the downregulation of the expression of anti-apoptotic proteins, such as Bcl-2 and survivin. In the present study, a subcutaneous mouse model was used to detect the antitumor efficacy of Cu(sal)(phen), which poses some limitations in evaluating antitumor efficacy. For example, the subcutaneous mouse model cannot fully simulate the progression and pathological changes of tumors in the colon, as tumor cells are inoculated under the skin, rather than in an orthotopic environment. In order to demonstrate the antitumor efficacy of Cu (sal) (phen) to a greater extent, we also attempted to conduct *in vivo* experiments using the SW480 cell xenograft model. However, the model of SW480 was not constructed well due to slow growth. Therefore, the authors aim to explore its potential in the treatment of CRC in more depth in future studies.

Acknowledgements

The authors would like to thank Dr David Xu from UCLA Health, California, CA, USA for critically reading the manuscript.

Funding

The present study was financially supported by the Huanghe Talented Scholar Grant of Wuhan City (no. 1010/06850002), the Jianghan University collaborative Innovation Grant (no. 3010/03100070), the Jianghan University Special Research Grant (no. 3015/08210002). J. Xu is a Chutian Scholar of the Department of Education, Jianghan University, Wuhan, China.

Availability of data and materials

The datasets used and/or analyzed during the current study are available from the corresponding author on reasonable request.

Authors' contributions

DW, WZ, YL and JX conceived and designed the experiments. ZL, LF, DN, MC and DW performed the experiments. ZL, DW, WZ, YL and JX analyzed the data. DW and JX wrote the manuscript. DW and JX confirm the authenticity of all the raw data. All authors reviewed the manuscript, and all authors have read and approved the final manuscript.

Ethics approvals and consent to participate

The animal experiments followed the rules of the Animal Ethics Committee of Jianghan University (Wuhan, China) and were performed in accordance with relevant guidelines and regulations, including the ARRIVE guidelines (ethics permission no. JHDXLL:2019-001).

Patient consent for publication

Not applicable.

Competing interests

The authors declare that they have no competing interests.

References

1. Sung H, Ferlay J, Siegel RL, Laversanne M, Soerjomataram I, Jemal A and Bray F: Global cancer statistics 2020: GLOBOCAN estimates of incidence and mortality worldwide for 36 cancers in 185 countries. CA Cancer J Clin 71: 209-249, 2021.
2. Lu WQ, Hu YY, Lin XP and Fan W: Knockdown of PKM2 and GLS1 expression can significantly reverse oxaliplatin-resistance in colorectal cancer cells. Oncotarget 8: 44171-44185, 2017.
3. Asadzadeh Z, Mansoori B, Mohammadi A, Kazemi T, Mokhtarzadeh A, Shanehbandi D, Hemmat N, Derakhshani A, Brunetti O, Safaei S, *et al*: The combination effect of Prominin1 (CD133) suppression and Oxaliplatin treatment in colorectal cancer therapy. Biomed Pharmacother 137: 111364, 2021.
4. Li Y, Sun Z, Cui Y, Zhang H, Zhang S, Wang X, Liu S and Gao Q: Oxaliplatin derived monofunctional triazole-containing platinum(II) complex counteracts oxaliplatin-induced drug resistance in colorectal cancer. Bioorg Chem 107: 104636, 2021.
5. Chen W, Lian W, Yuan Y and Li M: The synergistic effects of oxaliplatin and piperlongumine on colorectal cancer are mediated by oxidative stress. Cell Death Dis 10: 600, 2019.
6. Martinez-Balibrea E, Martínez-Cardús A, Ginés A, Ruiz de Porras V, Moutinho C, Layos L, Manzano JL, Bugés C, Bystrup S, Esteller M and Abad A: Tumor-related molecular mechanisms of oxaliplatin resistance. Mol Cancer Ther 14: 1767-1776, 2015.
7. Buchholz A, Sahmoun AE and Kurniali PC: Characteristics of colorectal patients who discontinued oxaliplatin therapy. J Clin Oncol 37 (Suppl): e15155, 2019.
8. Zedan AH, Hansen TF, Svenningsen ÅF and Vilholm OJ: Oxaliplatin-induced neuropathy in colorectal cancer: Many questions with few answers. Clin Colorectal Cancer 13: 73-80, 2014.
9. Ali A, Mishra S, Kamaal S, Alarifi A, Afzal M, Saha KD and Ahmad M: Evaluation of catacholase mimicking activity and apoptosis in human colorectal carcinoma cell line by activating mitochondrial pathway of copper(II) complex coupled with 2-(quinolin-8-yloxy)(methyl)benzonitrile and 8-hydroxyquinoline. Bioorg Chem 106: 104479, 2021.
10. Zehra S, Tabassum S and Arjmand F: Biochemical pathways of copper complexes: Progress over the past 5 years. Drug Discov Today 26: 1086-1096, 2021.
11. Song W, Xu P, Zhi S, Zhu S, Guo Y and Yang H: Integrated transcriptome and in vitro analysis revealed antiproliferative effects on human gastric cancer cells by a benzimidazole-quinoline copper(II) complex. Process Biochem 102: 286-295, 2021.
12. Sequeira D, Baptista PV, Valente R, Piedade MFM, Garcia MH, Morais TS and Fernandes AR: Cu(I) complexes as new antiproliferative agents against sensitive and doxorubicin resistant colorectal cancer cells: Synthesis, characterization, and mechanisms of action. Dalton Trans 50: 1845-1865, 2021.
13. Radhakrishnan K, Khamrang T, Sambantham K, Sali VK, Chitgupi U, Lovell JF, Mohammad AA and Venugopal R: Identification of cytotoxic copper(II) complexes with phenanthroline and quinoline, quinoxaline or quinazoline-derived mixed ligands. Polyhedron 194: 114886, 2021.
14. Mahendiran D, Kumar RS, Viswanathan V, Velmurugan D and Rahiman AK: Targeting of DNA molecules, BSA/c-Met tyrosine kinase receptors and anti-proliferative activity of bis(terpyridine) copper(ii) complexes. Dalton Trans 45: 7794-7814, 2016.
15. Gou Y, Chen M, Li S, Deng J, Li J, Fang G, Yang F and Huang G: Dithiocarbazate-copper complexes for bioimaging and treatment of pancreatic cancer. J Med Chem 64: 5485-5499, 2021.
16. Chen X, Dou QP, Liu J and Tang D: Targeting ubiquitin-proteasome system with copper complexes for cancer therapy. Front Mol Biosci 8: 649151, 2021.
17. Cui Q, Wang JQ, Assaraf YG, Ren L, Gupta P, Wei L, Ashby CR Jr, Yang DH and Chen ZS: Modulating ROS to overcome multidrug resistance in cancer. Drug Resist Updat 41: 1-25, 2018.
18. Snezhkina AV, Kudryavtseva AV, Kardymon OL, Savvateeva MV, Melnikova NV, Krasnov GS and Dmitriev AA: ROS generation and antioxidant defense systems in normal and malignant cells. Oxid Med Cell Longev 2019: 6175804, 2019.
19. Ng CH, Kong SM, Tiong YL, Maah MJ, Sukram N, Ahmad M and Khoo ASB: Selective anticancer copper(II)-mixed ligand complexes: Targeting of ROS and proteasomes. Metallomics 6: 892-906, 2014.
20. Polloni L, Seni Silva AC, Teixeira SC, Azevedo FVPV, Zóia MAP, da Silva MS, Lima PMAP, Correia LIV, do Couto Almeida J, da Silva CV, *et al*: Action of copper(II) complex with β-diketone and 1,10-phenanthroline (CBP-01) on sarcoma cells and biological effects under cell death. Biomed Pharmacother 112: 108586, 2019.
21. Pfeffer CM and Singh ATK: Apoptosis: A target for anticancer therapy. Int J Mol Sci 19: 448, 2018.
22. Banjara S, Suraweera CD, Hinds MG and Kvansakul M: The Bcl-2 family: Ancient origins, conserved structures, and divergent mechanisms. Biomolecules 10: 128, 2020.
23. Sun BB, Fu LN, Wang YQ, Gao QY, Xu J, Cao ZJ, Chen YX and Fang JY: Silencing of JMJD2B induces cell apoptosis via mitochondria-mediated and death receptor-mediated pathway activation in colorectal cancer. J Dig Dis 15: 491-500, 2014.
24. Li D, Hu C and Li H: Survivin as a novel target protein for reducing the proliferation of cancer cells. Biomed Rep 8: 399-406, 2018.
25. de Ridder I, Kerkhofs M, Veettil SP, Dehaen W and Bultynck G: Cancer cell death strategies by targeting Bcl-2's BH4 domain. Biochim Biophys Acta Mol Cell Res 1868: 118983, 2021.

26. Guvenc H, Pavlyukov MS, Joshi K, Kurt H, Banasavadi-Siddegowda YK, Mao P, Hong C, Yamada R, Kwon CH, Bhasin D, *et al*: Impairment of glioma stem cell survival and growth by a novel inhibitor for Survivin-Ran protein complex. Clin Cancer Res 19: 631-642, 2013.
27. Lopes JC, Botelho FV, Barbosa Silva MJ, Silva SF, Polloni L, Alves Machado PH, Rodrigues de Souza T, Goulart LR, Silva Caldeira PP, Pereira Maia EC, *et al*: In vitro and in vivo anti-tumoral activity of a ternary copper (II) complex. Biochem Biophys Res Commun 533: 1021-1026, 2020.
28. Fan L, Tian M, Liu Y, Deng Y, Liao Z and Xu J: Salicylate •phenanthroline copper (II) complex induces apoptosis in triple-negative breast cancer cells. Oncotarget 8: 29823-29832, 2017.
29. Sukhdeo K, Paramban RI, Vidal JG, Elia J, Martin J, Rivera M, Carrasco DR, Jarrar A, Kalady MF, Carson CT, *et al*: Multiplex flow cytometry barcoding and antibody arrays identify surface antigen profiles of primary and metastatic colon cancer cell lines. PLoS One 8: e53015, 2013.
30. Kreutz D, Bileck A, Plessl K, Wolrab D, Groessl M, Keppler BK, Meier SM and Gerner C: Response profiling using shotgun proteomics enables global metallodrug mechanisms of action to be established. Chemistry 23: 1881-1890, 2017.
31. Sun W, Ge Y, Cui JP, Yu YF and Liu BL: Scutellarin resensitizes oxaliplatin-resistant colorectal cancer cells to oxaliplatin treatment through inhibition of PKM2. Mol Ther Oncolytics 21: 87-97, 2021.
32. Guo WJ, Ye SS, Cao N, Huang JA, Gao J and Chen QY: ROS-mediated autophagy was involved in cancer cell death induced by novel copper(II) complex. Exp Toxicol Pathol 62: 577-582, 2010.
33. Cao Y, Wang J, Tian H and Fu GH: Mitochondrial ROS accumulation inhibiting JAK2/STAT3 pathway is a critical modulator of CYT997-induced autophagy and apoptosis in gastric cancer. J Exp Clin Cancer Res 39: 119, 2020.
34. Murphy MP: How mitochondria produce reactive oxygen species. Biochem J 417: 1-13, 2009.
35. Warren CFA, Wong-Brown MW and Bowden NA: BCL-2 family isoforms in apoptosis and cancer. Cell Death Dis 10: 177, 2019.
36. Peery RC, Liu JY and Zhang JT: Targeting survivin for therapeutic discovery: Past, present, and future promises. Drug Discov Today 22: 1466-1477, 2017.
37. Jiang F, Zhou JY, Zhang D, Liu MH and Chen YG: Artesunate induces apoptosis and autophagy in HCT116 colon cancer cells, and autophagy inhibition enhances the artesunate-induced apoptosis. Int J Mol Med 42: 1295-1304, 2018.
38. Schütz CS, Stope MB and Bekeschus S: H2A.X phosphorylation in oxidative stress and risk assessment in plasma medicine. Oxid Med Cell Longev 2021: 2060986, 2021.
39. Johnstone TC, Suntharalingam K and Lippard SJ: The next generation of platinum drugs: Targeted Pt(II) agents, nanoparticle delivery, and Pt(IV) prodrugs. Chem Rev 116: 3436-3486, 2016.
40. Gałczyńska K, Drulis-Kawa Z and Arabski M: Antitumor activity of Pt(II), Ru(III) and Cu(II) complexes. Molecules 25: 3492, 2020.
41. Wang NN, Zhang PZ, Zhang J, Wang HN, Li L, Ren F, Dai PF, Li H and Lv XF: Penfluridol triggers mitochondrial-mediated apoptosis and suppresses glycolysis in colorectal cancer cells through down-regulating hexokinase-2. Anat Rec (Hoboken) 304: 520-530, 2021.
42. Cui Q, Wen S and Huang P: Targeting cancer cell mitochondria as a therapeutic approach: Recent updates. Future Med Chem 9: 929-949, 2017.
43. Kleih M, Böpple K, Dong M, Gaißler A, Heine S, Olayioye MA, Aulitzky WE and Essmann F: Direct impact of cisplatin on mitochondria induces ROS production that dictates cell fate of ovarian cancer cells. Cell Death Dis 10: 851, 2019.
44. Xia S, Miao Y and Liu S: Withaferin A induces apoptosis by ROS-dependent mitochondrial dysfunction in human colorectal cancer cells. Biochem Biophys Res Commun 503: 2363-2369, 2018.
45. Kowol CR, Heffeter P, Miklos W, Gille L, Trondl R, Cappellacci L, Berger W and Keppler BK: Mechanisms underlying reductant-induced reactive oxygen species formation by anticancer copper(II) compounds. J Biol Inorg Chem 17: 409-423, 2012.
46. Basak D, Uddin MN and Hancock J: The role of oxidative stress and its counteractive utility in colorectal cancer (CRC). Cancers (Basel) 12: 3336, 2020.
47. Moloney JN and Cotter TG: ROS signalling in the biology of cancer. Semin Cell Dev Biol 80: 50-64, 2018.
48. Yang F, Pei R, Zhang Z, Liao J, Yu W, Qiao N, Han Q, Li Y, Hu L, Guo J, *et al*: Copper induces oxidative stress and apoptosis through mitochondria-mediated pathway in chicken hepatocytes. Toxicol In vitro 54: 310-316, 2019.
49. Tsvetkov P, Coy S, Petrova B, Dreishpoon M, Verma A, Abdusamad M, Rossen J, Joesch-Cohen L, Humeidi R, Spangler RD, *et al*: Copper induces cell death by targeting lipoylated TCA cycle proteins. Science 375: 1254-1261, 2022.
50. Piché A, Grim J, Rancourt C, Gómez-Navarro J, Reed JC and Curiel DT: Modulation of Bcl-2 protein levels by an intracellular anti-Bcl-2 single-chain antibody increases drug-induced cytotoxicity in the breast cancer cell line MCF-7. Cancer Res 58: 2134-2140, 1998.
51. Tanioka M, Nokihara H, Yamamoto N, Yamada Y, Yamada K, Goto Y, Fujimoto T, Sekiguchi R, Uenaka K, Callies S and Tamura T: Phase I study of LY2181308, an antisense oligonucleotide against survivin, in patients with advanced solid tumors. Cancer Chemother Pharmacol 68: 505-511, 2011.
52. Chen Y, Zhou Q, Zhang L, Zhong Y, Fan G, Zhang Z, Wang R, Jin M, Qiu Y and Kong D: Stellettin B induces apoptosis in human chronic myeloid leukemia cells via targeting PI3K and Stat5. Oncotarget 8: 28906-28921, 2017.
53. Niu D, Wang D, Fan L, Liu Z, Chen M, Zhang W, Liu Y, Xu J and Liu Y: The copper (II) complex of salicylate phenanthroline inhibits proliferation and induces apoptosis of hepatocellular carcinoma cells. Environ Toxicol 38: 1384-1394, 2023.